Critical Role of Ca^{2+} Ions in the Reaction Mechanism of *Euphorbia characias* Peroxidase†

Rosaria Medda,‡ Alessandra Padiglia,‡ Silvia Longu,‡ Andrea Bellelli,§ Alessandro Arcovito,§ Stefano Cavallo,§ Jens Z. Pedersen,|| and Giovanni Floris*,‡

Department of Applied Sciences in Biosystems, University of Cagliari, Department of Biochemical Sciences "A. Rossi Fanelli", University of Rome "La Sapienza", and CNR Center of Molecular Biology, Rome, Italy, and Department of Biology, University of Rome "Tor Vergata", Rome, Italy

Received April 16, 2003; Revised Manuscript Received June 3, 2003

ABSTRACT: A cationic peroxidase was isolated and characterized from the latex of the perennial Mediterranean plant *Euphorbia characias*. The purified enzyme contained one heme prosthetic group identified as ferric iron-protoporphyrin IX. In addition, the purified peroxidase contained 1 mol of endogenous calcium per mol of enzyme; removal of this calcium ion resulted in almost complete loss of the enzyme activity. However, when excess Ca^{2+} was added to the native enzyme the catalytic efficiency was enhanced by 3 orders of magnitude. The mechanism of activation was studied using a wide range of spectroscopic and analytic techniques. Analysis of the steady state by stopped-flow measurements suggests that the main effect of calcium ions is to favor the oxidation of the ferric enzyme by hydrogen peroxide to form compound I, whereas the other steps of the catalytic cycle seem to be affected to a lesser extent. UV/vis absorption spectra and CD measurements show that the heme iron is pentacoordinated high-spin in native enzyme and remains so after the binding of Ca^{2+}. Only minor changes in the secondary or tertiary structure of the protein could be detected by fluorescence or CD measurements in the presence of Ca^{2+} ions, except for a significant perturbation of the Fe^{3+} inner sphere geometry, as detected by EPR measurements. We propose that Ca^{2+} binding to a low affinity site induces a reorientation of the distal histidine changing the almost inactive form of *Euphorbia* peroxidase to a high activity form. This is the first example of a peroxidase that responds as an on/off switch to variations in the external Ca^{2+} level.

The superfamily of heme peroxidases isolated from many higher-order plants, fungi, and bacteria is a group of enzymes that utilizes hydrogen peroxide to oxidize a second reducing substrate (*1*). These enzymes are involved in the regulation of cell growth and differentiation, in cell wall lignification, and in the metabolism of hormones and alkaloids (ref *2* and references therein). Heme peroxidases can be grouped into three classes: class I contains bacterial and plant intracellular enzymes from mitochondria and chloroplasts, such as ascorbate peroxidase and cytochrome *c* peroxidase. Class II consists of secreted fungal peroxidases, for example, manganese peroxidase and lignin-degrading peroxidase. Class III contains secreted plant peroxidases exemplified by horseradish peroxidase (E.C. 1.11.1.7, donor: hydrogen peroxide oxidoreductase; HRP)[1] as the best known. There are more than 30 isoforms of HRP classified into three major groups: acidic, neutral, and basic forms. The horseradish peroxidase isozyme C, HRP-C, is the most studied isoform: it is a single glycosylated polypeptide chain of 308 residues with eight oligosaccharide side chains and a relative molecular mass of 33 900 (*3*). The native enzyme is generally considered to contain high-spin Fe^{3+} in a protoporphyrin IX pentacoordinated to a proximal histidine ligand. This histidine functions to stabilize the higher oxidation states of the iron atom (*4*), while another histidine, known as the distal, functions as an acid−base catalyst to accept one proton from the peroxide. Two mol of Ca^{2+}/mol of enzyme are also present in native HRP-C; the binding sites are known as the proximal and the distal site according to their location relative to the porphyrin plane. Ca^{2+} is also found in the other class II and III peroxidases, whereas class I cytochrome *c* peroxidase does not possess bound Ca^{2+} at all. The role of these ions has been intensively investigated, and in general Ca^{2+} has been proposed to maintain the heme pocket structure associated with high catalytic activities. Removal of the calcium ions in HRP-C, as well as in other class III peroxidases, results in changes in the electronic structure of the heme iron and in a considerable decrease in activity (*5*−*7*). Ca^{2+} acts as an activator of two isozymes of wheat peroxidase (*8*), and an activating effect of Ca^{2+} ions was shown in barley peroxidase, where the activity can be reversibly controlled by Ca^{2+}-induced conformational changes (*9, 10*). But although Ca^{2+} ions seem to be necessary for optimum catalysis of class III

† This study was partially supported by FIRB (Fondo per gli investimenti della ricerca di base) funds and by the C. N. R. Target Project on Biotechnology and Coordinated Project Agenzia 2000.

* To whom correspondence should be addressed. Tel: ++39-070-6754519. Fax: ++39-070-6754523. E-mail: florisg@unica.it.

‡ University of Cagliari.

§ Department of Biochemical Sciences "A. Rossi Fanelli", University of Rome "La Sapienza", and CNR Center of Molecular Biology.

|| University of Rome "Tor Vergata".

[1] Abbreviations: ABTS, 2,2′-azinobis(3-ethylbenzthiazoline-6-sulfonic acid); ELP, *Euphorbia* latex peroxidase; HRP, horseradish peroxidase; SDS−PAGE, sodium dodecyl sulfate polyacrylamide gel electrophoresis; Tris, tris-(hydroxymethyl)aminomethane.

10.1021/bi034609z CCC: $25.00
Published on Web 07/01/2003

enzymes, they are not essential for low levels of activity. This is at variance with the class II manganese peroxidase (*11*) in which the loss of either one or two Ca^{2+} ions rendered the enzyme inactive. The differences between the two classes of peroxidases were attributed to the different locations of intramolecular disulfide bridges.

We have previously isolated a cationic peroxidase from the latex of the Mediterranean shrub *Euphorbia characias* and reported some of its physicochemical characteristics (*12*). Surprisingly, the purified enzyme has a very low specific activity for classic peroxidase substrates when compared to HRP and other peroxidases. In the present paper, we show that the catalytic efficiency of this enzyme was enhanced by 3 orders of magnitude in the presence of Ca^{2+} ions. We have used this unique behavior to study the activation phenomenon by conventional and stopped-flow spectrophotometry and through comparison of the results with those reported for HRP-C, one of the typical peroxidases**,** and we present a possible explanation of the mechanism of activation.

EXPERIMENTAL PROCEDURES

Materials. HRP (RZ value $A_{403}/A_{280} = 3.2$), ABTS, *o*-dianisidine, and ascorbic acid were purchased from Sigma (St. Louis, MO). Hydrogen peroxide was from Merck (Darmstadt, Germany), and an $\epsilon_{240} = 43.6\ M^{-1}\ cm^{-1}$ was used to determine its concentration. All chemicals were obtained as pure commercial products and used without further purification.

Enzyme. Peroxidase from *E. characias* latex (ELP; RZ value = 2.7) was purified as previously described (*12*). The latex was drawn from cut branches of *E. characias* and collected in glass containers. ELP was purified as the following steps (for details, see ref *12*). Step 1: acetone powder. Step 2: crude extract. Step 3: dialysis against deionized water. Step 4: ammonium sulfate fractionation. Step 5: DEAE-cellulose chromatography. Step 6: hydroxyapatite column chromatography. Step 7: SP-Sephadex column chromatography.

Gel Chromatography. Gel chromatography was carried out at 4 °C using a column (2.5 × 90 cm) of Sephacryl S-200 High Resolution (Pharmacia Biotech, Uppsala, Sweden) equilibrated and eluted with 100 mM potassium-phosphate buffer, pH 7, containing 300 mM KCl. The distribution coefficient (K_d) was obtained as described (*13*). The protein standards were catalase, aldolase, bovine serum albumin, and ovalbumin.

Metal and Heme Content. The presence of metals was measured by atomic absorption using a Unicam 969 AA spectrometer Solar (Bournemouth, Dorset, UK). The heme content was determined from the absorption spectra of the oxidized and reduced forms of the pyridine hemochromogen derivative, assuming a differential absorption coefficient of $\Delta\epsilon_{541}$ (for the dithionite-reduced enzyme) − $\Delta\epsilon_{557}$ (for the ferricyanide-oxidized enzyme) = $20.7\ mM^{-1}\ cm^{-1}$ (*14*).

Deglycosylation Analysis. Protein samples were denaturated by boiling for 5 min and then deglycosylated with *N*-glycosidase (5 μg/mL) in 50 mM sodium-phosphate buffer, pH 7.2, at 37 °C for 12 h. Controls were performed in samples without *N*-glycosidase. For M_r determination, proteins were analyzed on SDS−PAGE.

Peroxidase Activity. Activity measurements were performed in 100 mM sodium-acetate buffer, pH 5.75, and 25 °C, using hydrogen peroxide and the reducing substrate ABTS by following the increase in absorbance at 415 nm resulting from the formation of the ABTS cation radical product ($\epsilon_{415} = 36\ mM^{-1}\ cm^{-1}$). The activity was also determined by measuring the change in absorbance at 460 nm because of *o*-dianisidine oxidation. Activity was calculated in standard enzyme units (μmol min^{-1} mg^{-1}), and catalytic-center activity (k_{cat}) was defined as (mol of substrate consumed)/(mol of active sites) in 1 s. The value of K_M for ELP using varying reducing-substrate concentrations at a saturating concentration of hydrogen peroxide (25 mM), or varying concentrations of hydrogen peroxide at a saturating concentration of reducing substrate (10 mM ABTS), was calculated from double reciprocal plots by Michaelis−Menten analysis in 100 mM sodium-acetate buffer, pH 5.75, the optimum pH found for ELP. The k_{cat}/K_M value, a more useful measure of substrate specificity, was compared to that obtained for HRP. The effect of pH on ELP activity was tested in 100 mM sodium-acetate and Tris/HCl buffers. The effects of Ca^{2+} ions on ELP activity were examined in buffers with or without $CaCl_2$ or with $CaCO_3$ or chlorides of different metals to distinguish the specific effects of the various ions.

K_i and K_d Determination of Cyanide Binding. The affinity of ferric ELP for cyanide, a competitive inhibitor of heme containing enzymes, was determined by taking advantage of the characteristic absorbance changes associated with coordination to the heme iron. The data so obtained were compared with the inhibition constants determined from the effect of cyanide on the steady-state parameters. Titrations were made at 25 °C in 100 mM Tris/HCl buffer, pH 7.0, or in 100 mM sodium-acetate buffer, pH 5.75, in the presence or absence of 10 mM Ca^{2+} ions, by stepwise addition to an ELP solution of 5 μL (1.5 nmol) freshly prepared cyanide reagent to the ELP solution, and the optical density changes were measured at the appropriate wavelength 15 min after each addition (see Results). Inhibition constants were determined from Dixon plots (*15*). The determination of cyanide affinity from steady-state experiments is unequivocal, given the very low concentration of the enzyme employed in these experiments. Moreover, direct spectroscopic determinations cannot be carried out at enzyme concentrations lower than 1−3 μM (i.e., in these experiments the total and free cyanide concentrations differ to a significant extent). The mass law yields $[E\text{-}CN]/[E_t] = [CN^-]/K_d + [CN^-]$. Taking into account the total concentrations of cyanide ($[CN^-]_t$) and ELP ($[E]_t$), and the relationships $[CN^-] = [CN^-]_t - [E\text{-}CN]$ and $[E] = [E]_t - [E\text{-}CN]$, we obtain the following equation, whose solution was fed to the minimization routine:

$$[E\text{-}CN]^2 - [E\text{-}CN]([CN^-]_t + [E]_t + K_d) + [CN^-]_t[E]_t = 0$$

Spectrophotometry. Absorption spectra and data from all activity assays were obtained with an Ultraspec 2000 spectrophotometer (Pharmacia Biotech Ltd., Cambridge, UK) using 1 cm light-path cells.

Fluorescence Spectra. Fluorescence spectra were obtained using a Perkin-Elmer LS-3 spectrofluorimeter (Perkin-Elmer Ltd., Buckinghamshire, UK).

Circular Dichroism Spectroscopy. CD spectra were measured with a Jasco J-715 spectropolarimeter (Jasco, Hachioji City, Tokio, Japan). A 9.2 μM solution of ELP in 100 mM Tris/HCl buffer, pH 7.0, was placed in strain free 0.1 mm (for far UV spectra) and 1.0 cm (for Soret spectra) quartz cuvettes, and spectra were measured between 260 and 190 nm or 460 and 350 nm with the following setup: bandwidth 2 nm, time constant 2 s, scan rate 20 nm/min, and N_2 purging rate 25 L/min. A total of eight spectra corrected for background (phosphate buffer and salt) were averaged and successively smoothed with an eight points Savisky Golay smoothing procedure. The CD spectrum was normalized as $\Delta\epsilon$ units using the molar extinction coefficient $\epsilon_{280} = 3 \times 10^4\ M^{-1}\ cm^{-1}$.

Stopped-Flow Experiments. Stopped-flow experiments were carried out using an Applied Photophysics MV 17 apparatus (Leatherhead, UK), equipped with a 1 cm light-path observation chamber and either a monochromator and a photomultiplier tube (for single wavelength measurements) or a spectrometer and a photodiode array detector (for rapid acquisition of absorbance spectra over the range of 250−800 nm). Single wavelength measurements were analyzed by a least squares minimization routine (developed using the Borland Pascal 7.0 compiler) capable of fitting to the experimental data of any desired theoretical model using either analytical or numerical integration. Time-resolved absorption spectra were deconvoluted by a singular value decomposition performed with the program MATLAB (The Math Works, Natick, MA). This analysis requires the time-resolved spectra to be arranged into matrix A, each column being a spectrum and each row a time course or a titration profile at a single wavelength. The application of SVD yields three matrixes, **U**, **S**, and **V**, such that $\mathbf{A} = \mathbf{USV}^T$. **U** and **V** are orthogonal matrixes, whereas **S** is diagonal, its nonzero elements arranged in decreasing order. Each column of matrix **US** represents a pseudospectrum (i.e., the absorption of one of the spectroscopic components required to approximate the original data, and only the first few columns are significant, the last ones corresponding to negligibly small **S** values). Each column of matrix **V** represents the time course or titration profile of the corresponding column of **US** and was analyzed by ordinary nonlinear minimization routines (by using either MATLAB or dedicated programs developed with the Borland Pascal Compiler) as already described (*16*), to obtain the pertinent equilibrium or kinetic constants and the amplitudes of the **V** elements. The fitted **V** amplitudes ($\mathbf{V}_{fit}$) were used to calculate the spectra of each chemical species involved in the reaction in accordance with the formula: $\mathbf{A}_{fit} = \mathbf{USV}_{fit}^T$.

Laser Photolysis Experiments. Laser photolysis experiments were carried out using an instrument developed in our laboratory (*17*). Briefly, the 5 ns pulse of a Nd:YAG laser (Quanta Systems, Milan, Italy; we used the second harmonic with a wavelength of 532 nm and $E = 10$ to 100 mJ/pulse) was focused onto one face of a 1 cm fluorescence cuvette sealed to a Thunberg tube containing the desired solution and gas phase. The transmittance of the sample was monitored by an optical line arranged at 90° with respect to the laser pulse, consisting of a 100 W lamp (Oriel, Stratford, CT), a blue glass filter (Corning Glassware, Corning, NY), the sample holder, a second filter, a monochromator (Spex, Edison, NJ), and a photomultiplier module (model H6870 by Hamamatsu, Shimokanzo, Shizuoka-ken, Japan). The output current of the photomultiplier was converted to voltage by a Tektronix ADA400 amplifier and read in a Tektronix TDS360 digital oscilloscope (Tektronix, Beaverton, OR). The use of a faster current to voltage amplifier (model AM3100 by Analogue Modules USA, capable of time resolution up to 350 MHz) allowed us to explore the nanosecond and microsecond time regime. However, no spectroscopic changes could be detected in this time window; therefore, no such data are presented in this work.

Electron Spin Resonance Spectra. ESR spectra were recorded with a Bruker ESP 300 instrument (Karlsruhe, Germany) using a standard TE_{102}-type cavity for low-temperature Fe^{III} measurements. Samples of 300 μL in 3 mm i.d. quartz tubes were measured at 100 K. ESR spectra were recorded at 1 or 10 mW microwave power, using 0.1 or 1 mT modulation amplitude.

RESULTS

Characterization of Euphorbia Peroxidase. Since plant peroxidases may exist in numerous molecular forms, we used electrophoresis under nondenaturing conditions and isoelectric focusing to single out all the possible isoform species. Peroxidase bands were visualized with the *o*-dianisidine/hydrogen peroxide method. It was not possible to detect any protein bands by PAGE or isoelectric focusing using directly the thick white latex, probably because of interference because of its composition. The analysis of the isoform species was therefore only made after the acetone powder step (step 1). No isoenzyme species could be detected by PAGE or by analytical gel electrofocusing in the pH ranges of 3−10 and 5−8. SDS−PAGE of purified ELP showed a single band with a M_r of 46 000 ± 1000, whereas gel filtration chromatography gave a M_r of 47 000. We analyzed the extent of glycosylation in *Euphorbia* latex peroxidase treating denatured protein samples with *N*-glycosidase. Comparing the mobility with that of untreated controls revealed a significant shift in molecular mass from 46 000 to 39 000 (not shown), suggesting that the protein may contain about 15% carbohydrate. The isoelectric pH of ELP was found to be 7.4.

The purified enzyme contained 0.12% (w/w) iron corresponding to an Fe/protein ratio of 1:1 and a heme prosthetic group that was identified as ferric iron-protoporphyrin IX. The purified ELP also contained 1 mol of endogenous calcium per mol of enzyme; this strongly bound calcium could be removed by incubating the enzyme in 100 mM Tris/HCl buffer, pH 7.2, for 18 h at 25 °C with 6 M guanidine hydrochloride and 10 mM EDTA and extensive dialysis in water (*5*), as confirmed by atomic absorption measurements. The final absorbance of the Soret band was about 70% of that of the native protein, probably because of incomplete heme capture during refolding. The activity of the Ca^{2+}-free enzyme was approximately 2% of the native enzyme (results not shown).

Reaction of ELP with Hydrogen Peroxide and Reducing Substrates: Kinetics Parameters. The effect of pH on ELP activity was tested in sodium-acetate and Tris/HCl buffers using ABTS as substrate. The pH curve showed an optimum at 5.75 (Figure 1). The value of K_M for ABTS at a saturating concentration of hydrogen peroxide was shown to be of the

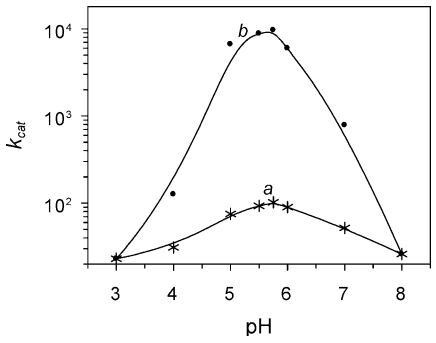

FIGURE 1: Effect of pH on *Euphorbia* peroxidase activity. The buffers used were 100 mM sodium-acetate, pH 3−6, and 100 mM Tris/HCl, pH 7−8. (a) Purified enzyme and (b) enzyme in the presence of 10 mM Ca^{2+} ions. k_{cat} = (mol of substrate consumed)/(mol of active sites) in 1 s. Data reported are calculated as the mean of at least five different measurements.

Table 1: Kinetics Parameters of Horseradish Peroxidase (HRP) and *Euphorbia* Latex Peroxidase (ELP) and of ELP in the Presence of 10 mM Ca^{2+} Ions[a]

	HRP	ELP	ELP-Ca^{2+}
K_M ABTS[b] (mM)	0.88 ± 0.092	1.1 ± 0.12	0.33 ± 0.03
k_{cat}[b,c] (s^{-1})	890 ± 98	102 ± 14	10200 ± 936
k_{cat}/K_M ABTS (mM^{-1} s^{-1})	1010	93	30900
K_M H_2O_2[c] (mM)	0.022 ± 0.004	2.6 ± 0.37	0.27 ± 0.032
k_{cat}/K_M H_2O_2 (mM^{-1} s^{-1})	40450	39	37700

[a] Buffer used: 100 mM sodium-acetate buffer, pH 5.75. [b] Using saturating concentrations of H_2O_2 (25 mM). [c] Using saturating concentrations of ABTS (10 mM).

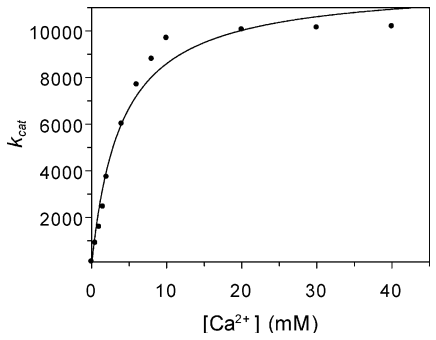

FIGURE 2: Effect of the Ca^{2+} concentration on *Euphorbia* peroxidase activity. The buffer used was 100 mM sodium-acetate, pH 5.75. The continuous curve represents the theoretical binding isotherm fit to the data.

same order of magnitude for HRP and ELP (Table 1), whereas the K_M for hydrogen peroxide at a saturating concentration of ABTS was calculated to be 0.022 and 2.6 mM for HRP and ELP, respectively. ELP showed a k_{cat} value approximately 9 times lower than that found for HRP. A very small k_{cat}/K_M value for ELP, as compared with that found for HRP, was seen for hydrogen peroxide, whereas the k_{cat}/K_M value for ABTS in the *Euphorbia* enzyme was about 11% of that found for HRP.

Effect of Ca^{2+} on the Enzyme Activity. The effect of added Ca^{2+} ions on ELP activity was investigated using ABTS as substrate. When native ELP was incubated for 10 min in the presence of Ca^{2+}, a drastic activation was observed (Table 1; Figure 2), which showed a maximum at 10 mM Ca^{2+} ion concentration. Since ABTS might bind divalent metal ions, these experiments were also carried out with the substrate *o*-dianisidine giving the same results as obtained with ABTS (data not shown). The activation by Ca^{2+} ions was strongly pH-dependent. As shown in Figure 1, 100-fold activation was observed in the presence of 10 mM Ca^{2+} in sodium-acetate buffer, pH 5.75. At pH 4.5 and 8, very little activity (if any) could be measured. After dialysis against 100 mM Tris/HCl or sodium-acetate buffers or filtration through a Sephacryl S-200 column, the activating effect was lost. The dissociation constant (K_d) for the binding of Ca^{2+} at fixed saturating concentrations of reducing substrate (ABTS, 10 mM) and hydrogen peroxide (25 mM) was calculated to be 3.5 mM.

The data reported in Figure 2 are consistent with the binding of 1 additional mol of Ca^{2+} ion per mol of *Euphorbia* peroxidase, as suggested by analyzing the dependence of k_{cat} on the concentration of Ca^{2+}, according to the equation $n Ca^{2+} = \Delta \log k_{cat}/\Delta \log [Ca^{2+}]$ (*18*, *19*). The use of this equation is justified if the enzyme activity is tested under saturating concentrations of both substrates. It is important to state that this equation would not detect a stoichiometry higher than 1:1 if the binding sites were perfectly equivalent and independent of each other, but this hypothesis is unlikely in a monomeric hemoprotein.

Other Ionic Effects. Similar activation to that obtained with $CaCl_2$ was seen in the presence of $CaCO_3$. No effect of Cl^- was observed. Other divalent cations such as Sr^{2+} and Ba^{2+} gave rise to minor activation of the enzyme (20 and 10 times, respectively, at 10 mM concentration), whereas Mg^{2+} and Mn^{2+} had no effect on ELP activity.

Mechanism of Activation of ELP by Ca^{2+}. The catalytic cycle of HRP-C and other peroxidases is well-established (*20*−*26*) and is briefly summarized here to facilitate the description of the results obtained. The initial reaction of hydrogen with HRP forms a ferric hydroperoxide, the compound 0 (*25*, *27*), the distal histidine acting as a general base. The transiently protonated histidine then acts as a general acid to protonate the leaving hydroxide and generate a green enzyme intermediate compound I, with both of the oxidizing equivalents of H_2O_2 transferred to the enzyme. One of the two oxidizing equivalents of peroxide is accounted for by the loss of an electron from the iron atom that is oxidized to a ferryl complex in compound I ($Fe^{IV} = O^{2-}$), whereas the second electron is donated by the porphyrin ring, oxidized to a π-cation radical. Compound I then reverts to the resting state by two successive one-electron reactions with reducing substrate molecules (DH_2). The red compound II, a second enzyme intermediate, is produced by the first electron transfer of DH_2 to compound I. The reaction proceeds through the following mechanism:

$$\mathrm{HRP(PrIXFe^{III}) + H_2O_2} \xrightarrow{k_1} \mathrm{compound\ I(PrIX^{\bullet+}Fe^{IV} = O) + H_2O} \quad (1)$$

$$\mathrm{compound\ I + DH_2} \xrightarrow{k_2} \mathrm{compound\ II(PrIXFe^{IV} = O) + DH^{\bullet} + H^+} \quad (2)$$

$$\mathrm{compound\ II + DH_2} \xrightarrow{k_3} \mathrm{HRP + DH^{\bullet} + OH^-} \quad (3)$$

$$\mathrm{DH^{\bullet} + DH^{\bullet} = D + DH_2} \quad (4)$$

With a large excess of H_2O_2 and in the absence of reducing substrates, peroxidases may decompose hydrogen peroxide

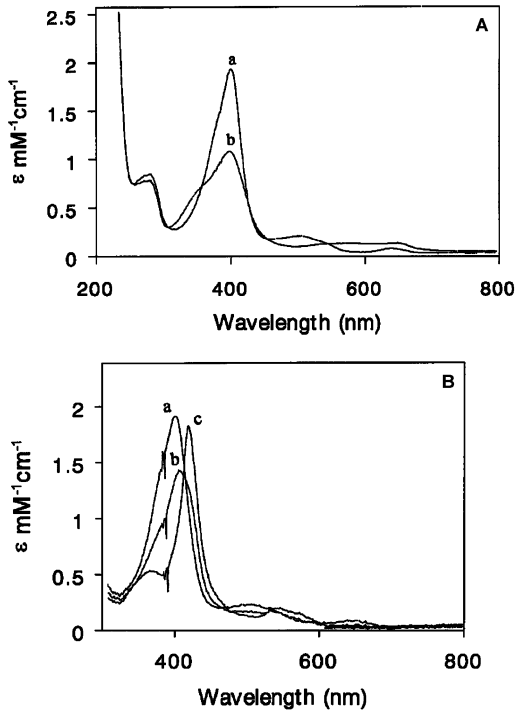

FIGURE 3: (A) Absorption spectra of *Euphorbia* peroxidase. (a) native peroxidase (15 μM) and (b) compound I obtained as reported in Experimental Procedures. (B) *Euphorbia* peroxidase in the presence of CN^- and 10 mM Ca^{2+} ions in 100 mM sodium-acetate buffer, pH 5.75. (a) native peroxidase (15 μM), (b) the same in the presence of 7.5 nmol of CN^-, and (c) in the presence of 15 nmol of CN^-.

to oxygen and water. These conditions may also result in the formation of oxygen radicals that inactivate the enzyme. The inactive compound III, or oxyperoxidase, is obtained (*28*). Trapped species of HRP compounds I and II, as well as several ferric derivatives, have been reported using X-ray absorption studies at low temperature (*29*).

Spectrophotometric Features. The electronic absorption spectrum of ELP showed maxima at 278, 401, 498, and 637 nm in 100 mM potassium-phosphate buffer, pH 7 (Figure 3A). The compound I with characteristic absorption maxima at 278, 398, 544, 577, and 651 nm was achieved by pretreating the enzyme with equimolar amounts of hydrogen peroxide for 24 h at 25 °C (*26*). Then, an additional equimolar amount of hydrogen peroxide was added for 15 min at 3 °C (Figure 3A). Compound II with characteristic absorption maxima at 278, 413, 541, and 576 nm was generated from compound I by the addition of 1 equiv of ascorbic acid (not shown; ref *30*). From 270 to 700 nm the spectra of compounds I and II were similar to those already reported for HRP (*31*); the absorbance spectra in the presence of 10 mM Ca^{2+} ions were very similar, and similar spectra were also obtained in 100 mM sodium-acetate buffer, pH 5.75. The related millimolar extinction coefficients of the native enzyme, compounds I and II, are reported in Table 2.

Formation of the Cyanide Derivative. CN^- behaved as a competitive inhibitor of ELP. At pH 5.75 and 7, the K_i values were calculated to be 6 and 2 μM, respectively. In the presence of 10 mM Ca^{2+} ions, only the K_i value at the lower pH changed markedly to 1 μM. The extinction coefficients of the adduct ELP-CN^- are reported in Table 2. It is well-known that the cyanide adduct may be compared to the initial binding of hydrogen peroxide to peroxidases (*32*). To analyze

Table 2: Extinction Coefficients of Native *Euphorbia* Latex Peroxidase, Compounds I and II, and the ELP-CN Derivative in 100 mM Sodium-Acetate Buffer, pH 5.75

native ELP ϵ (mM^{-1} cm^{-1})	compound I ϵ (mM^{-1} cm^{-1})	compound II ϵ (mM^{-1} cm^{-1})	ELP-CN^- ϵ (mM^{-1} cm^{-1})
$\epsilon_{278} = 66.7$			
$\epsilon_{401} = 130.7$	$\epsilon_{398} = 80.6$	$\epsilon_{413} = 120.5$	$\epsilon_{418} = 138$
$\epsilon_{458} = 16.3$		$\epsilon_{541} = 15$	
$\epsilon_{637} = 5.15$	$\epsilon_{651} = 9$	$\epsilon_{577} = 12.6$	

the influence of Ca^{2+} ions on the binding of cyanide, ELP was titrated with CN^- in the presence or absence of 10 mM Ca^{2+} in 100 mM sodium-acetate buffer, pH 5.75, and in 100 mM Tris/HCl buffer, pH 7. When CN^- was added to 15 μM ELP, the absorption band at 401 nm disappeared in parallel with formation of a band at 418 nm (Figure 3B). In this process, isosbestic points at 460 and 535 nm were observed. Cyanide titration of ELP showed that the binding of cyanide was markedly changed in the presence of 10 mM Ca^{2+} ions. K_d was found to be 1.9 and 5.6 μM in the presence and absence of Ca^{2+}, respectively, at pH 5.75, and 2.1 and 2.5 μM, respectively, at pH 7 (not shown). These results agree closely with those obtained by measuring the inhibitory effect of cyanide on the steady-state parameters. Moreover, the effect of Ca^{2+} ions on the dissociation constants of cyanide reflects the activation effect, which is greater at pH 5.75 than at pH 7 (Figure 1).

Stopped-Flow Determinations. Two types of experiments were carried out to investigate the fundamental steps of the catalytic cycle of ELP. First, the resting ferric enzyme was mixed with hydrogen peroxide in the absence of the reducing substrate. Second, the enzyme was mixed with hydrogen peroxide and ascorbate; by repeating this experiment several times over some minutes, we checked that H_2O_2 was not consumed by ascorbate while waiting in the instrument. Both experiments were carried out at several concentrations of each substrate in the presence or absence of calcium ions (Figure 4). In the presence of calcium ions, ELP reacted rapidly with hydrogen peroxide to yield the compound I product. When H_2O_2 was present in stoichiometric amounts, and was thus completely consumed in the reaction, compound I was stable at least over the time scale explored (i.e., up to several minutes). When the concentration of hydrogen peroxide exceeded that of the enzyme, at least one further reaction took place, the product of which is called X in Scheme 2.

In the absence of calcium ions, a different behavior was observed since the formation of compound I was very slow and this intermediate did not accumulate but was converted into X almost as soon as it was formed (Figure 4B). Comparison of the time courses of the reaction with H_2O_2 reveals the striking effect of calcium, which increases the second-order rate constant by a factor of 100 or more (Table 3).

The catalytic cycle, with its pre-steady-state processes, could be studied in the experiments carried out by mixing ferric ELP with both its substrates (H_2O_2 and ascorbate). These experiments show a characteristic fall and rise in absorbance, with an evident flat region, corresponding to the steady-state phase (Figure 4). An obvious and model independent observation is that the fast process of the reaction with H_2O_2 observed in the presence of Ca^{2+} is compatible

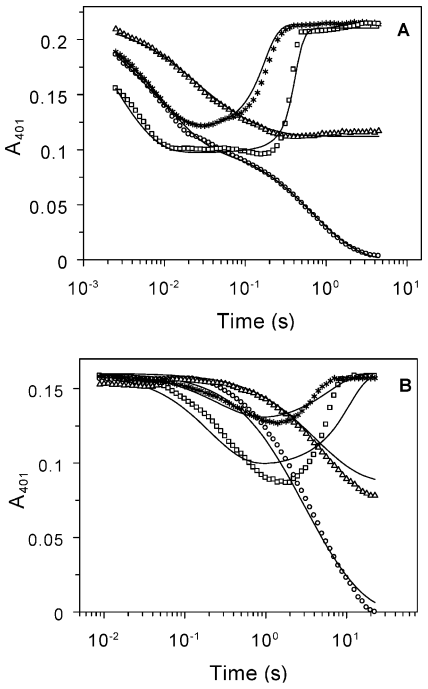

FIGURE 4: Time course of the absorbance changes recorded at 401 nm in the presence (A) or absence (B) of 10 mM calcium ions. Experimental conditions: 100 mM sodium-acetate buffer, pH 5.75, 20 °C, and ELP concentration 3.6 μM (after mixing). The concentration of substrates (after mixing) are as follows: hydrogen peroxide 3.3 μM (△); hydrogen peroxide 10 μM (○); hydrogen peroxide 10 μM and sodium ascorbate 100 μM (*); and hydrogen peroxide 25 μM and sodium ascorbate 100 μM (□). The continuous curves were calculated using the constants given in Table 3.

Scheme 1

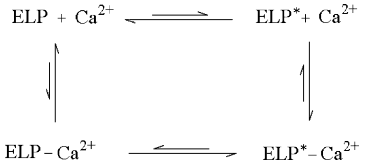

Scheme 2

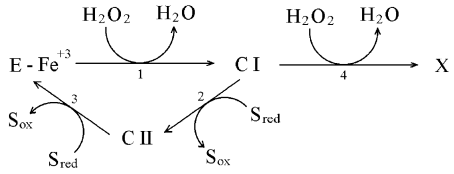

Table 3: Kinetic Rate Constants Describing the Steady State of the ELP-Catalyzed Oxidation of Ascorbate by H_2O_2[a]

	k_1 ($M^{-1}\,s^{-1}$)	k_2 ($M^{-1}\,s^{-1}$)	k_3 ($M^{-1}\,s^{-1}$)	k_4 ($M^{-1}\,s^{-1}$)
ELP (native enzyme)	7.7×10^4	1.3×10^7	2.8×10^4	3.2×10^4
ELP + 10 mM Ca^{2+} ions	1.2×10^7	1.2×10^7	3.0×10^5	2.5×10^5

[a] Experimental conditions as in Figure 4. All the kinetic processes of the model employed to fit the experimental data are second order (see Scheme 2).

with the steady state (compare the time course indicated by circles in Figure 4A with that indicated by asterisks). The same cannot be said of the experiments carried out in the absence of Ca^{2+} (Figure 4B) where the reaction observed in the absence of ascorbate is too slow to be relevant for the steady state.

Even an incomplete interpretation of the steady state, however, requires a kinetic model of the catalytic cycle and cannot be model independent. The catalytic mechanism of peroxidases is complex, but under appropriate experimental conditions (i.e., when the concentration of H_2O_2 is low and that of the reducing substrate is high), it is possible to limit the number of significantly populated intermediates to three (i.e., the resting ferric enzyme and compounds I and II). The experiments presented in this paper were analyzed using a modification of this minimum catalytic cycle (Scheme 2), which further contains the intermediate called X. This intermediate is populated mostly or exclusively in those experiments in which the resting ferric enzyme was allowed to react with hydrogen peroxide in the absence of the reducing substrate. The catalytic mechanism depicted in Scheme 2 satisfactorily describes the reaction of ELP in the presence of calcium but fails to describe the absorbance changes recorded in the absence of this ion (Figure 4). We did not attempt to analyze the latter data with more complex models since the low enzyme activity may favor the population of several intermediates, giving rise to multiple and complex alternative reaction pathways. Therefore, for the time being, we limit our analysis to the statement that the catalytic mechanism depends on the presence of calcium ions.

Although the species X could not be identified with certainty, some of its properties were evident from the experiments reported in Figure 4. X was formed only when an excess of H_2O_2 was present and a reducing substrate was absent. On longer time scales than those explored by stopped flow it disappeared. Moreover, this intermediate X was not identical to the dark-red compound III [Fe(II)-O_2], which could be formed upon addition of a 25-fold excess of hydrogen peroxide to the native ELP (not shown). As a working hypothesis, we suggest that the species X may be an intermediate of ELP with a very low catalase-like activity.

Interpretation of the stopped-flow experiments using the Scheme 2 yielded the rate constants reported in Table 3 and the continuous curves shown in Figure 4. Although other, more complex, kinetic schemes may also describe our data (and actually may better describe those collected in the absence of calcium as reported in Figure 4B), deciding among them would be arbitrary; thus, we prefer the minimal Scheme 2. Three main points are provided by this analysis: (i) compound I forms quickly in the presence of Ca^{2+} ions and slowly in the absence, but in both cases it does not accumulate since it is rapidly converted to compound II: ascorbate reacts quickly with compound I and prevents the formation of X; (ii) in the presence of Ca^{2+} ions, the rate-limiting step is the reduction of compound II to the ferric enzyme, as is usual for peroxidases; on the other hand, in the absence of Ca^{2+} ions, either k_1 or k_3 may be rate limiting, depending on the concentrations of the two substrates; this is very unusual in peroxidases; and (iii) Ca^{2+} ions affect only or mostly the first step of the catalytic cycle.

Laser Photolysis Experiments. Euphorbia peroxidase, reduced with sodium dithionite, was equilibrated with CO and submitted to flash photolysis. The rate of CO recombination was measured at pH 5.75 (Figure 5A) and at pH 7 (Figure 5B), in the absence and in the presence of $CaCl_2$ (5 and 10 mM). Exploration of faster time regimes, down to the tens of nanoseconds, revealed neither geminate rebinding

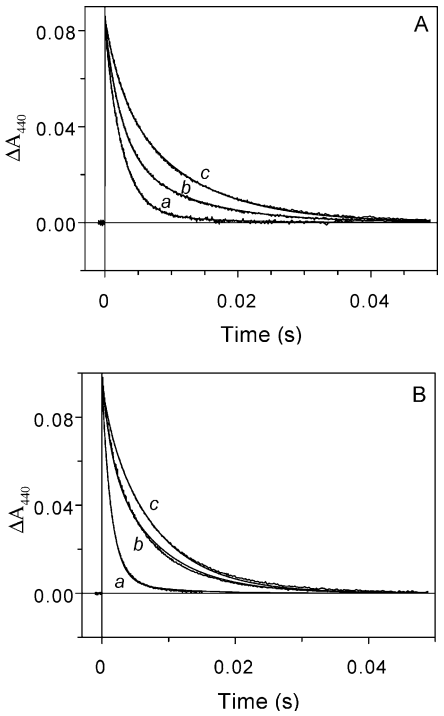

FIGURE 5: Time course of CO recombination as observed after photolysis of the peroxidase−CO complex. Experimental conditions: 100 mM sodium-acetate buffer, pH 5.75 or 100 mM Tris/HCl buffer, pH 7; temperature 20 °C; ELP concentration 3.4 μM; and observation wavelength 440 nm. ELP was reduced by adding a few grains of sodium dithionite to a sample already equilibrated with CO. (A) pH 5.75. (B) pH 7; line (a) without Ca^{2+}; line (b) in the presence of 5 mM Ca^{2+} ions; and line (c) in the presence of 10 mM Ca^{2+} ions.

Table 4: Kinetic Rate Parameters Describing the CO Combination to Ferrous ELP in Sodium Acetate and Tris/HCl Buffers[a]

pH	k_1 ($M^{-1}s^{-1}$)	k_2 ($M^{-1}s^{-1}$)	% SRF (without Ca^{2+})	% SRF (5 mM Ca^{2+})	% SRF (10 mM Ca^{2+})
5.75	4.1×10^5	9×10^4	6.0	37	68
7	7.2×10^5	1.3×10^5	6.7	64	86

[a] The time courses recorded at 440 nm and 1 atm CO were fitted to two pseudo-first-order processes, described by the rate constants k_1 and k_2, which are independent of calcium. The percentage of the absorbance change assigned to the slower process (% slowly reacting form, SRF) increases as calcium is added. Thus, the effect of this ion is to shift the equilibrium between the quickly and the slowly reacting forms of the enzyme (see text).

of CO nor other optical transitions as those assigned to conformational rearrangements in other hemoproteins (*33*). The time courses recorded at 440 nm at each pH value could be described by two parallel exponential decays with common rate constants and whose relative amplitude depended on the concentration of calcium ions (Table 4). This finding was compatible with the hypothesis that the enzyme molecule may assume either of two alternative structural conformations with different CO reactivities; the equilibrium between the two conformations was slow as compared with the recombination of CO, at least under our experimental conditions (i.e., 1 atm CO; overall half time of recombination approximately 5 ms). The binding of calcium ions changed the equilibrium toward the slowly reacting form. From the data reported in Table 4, it was possible to estimate the equilibrium dissociation constant of calcium, which was 7.6 mM at pH = 5.75 and 2.6 mM at pH = 7, consistent with

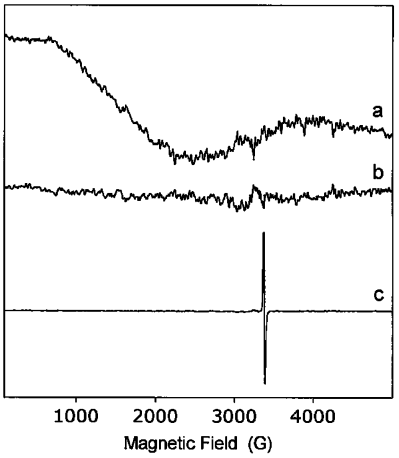

FIGURE 6: ESR spectra of ELP measured at 100 K, in the presence (a) or absence (b) of 10 mM Ca^{2+} and after addition of 10 mM Ca^{2+}, 8 μM H_2O_2, and 1 mM ABTS (c). The enzyme concentration was 3.4 μM, and the buffer was 100 mM sodium-acetate, pH 5.75.

the affinities measured in steady-state experiments. Since ions usually combine quickly with proteins, it is unlikely that the equilibrium of calcium binding and release was reached so slowly that it could not compete with the recombination of CO. In our opinion, it is more likely that, even if calcium is quickly bound (or released) as a consequence of photolysis, the structural transition of the protein lags behind the rebinding of CO.

Electron Spin Resonance Spectroscopy. The heme iron of ELP is believed to be a paramagnetic Fe(III) species in the resting state, as in the other class III peroxidases, and should therefore be ESR active. ESR spectra of native ELP measured at 100 K did not show any signals (Figure 6, line b), but this is in fact normal for hemoproteins and is most likely because of a too fast relaxation of the iron (*34*). However, when Ca^{2+} was added to the sample, a broad band appeared in the low-field region of the spectrum (Figure 6, line a); the position of this signal corresponded to that expected for a peroxidase, with a g value close to 6.0. This indicated a reduced relaxation rate of the iron, consistent with a minor change in the geometry of the ligand field. Given the fixed equatorial arrangement of the four porphyrin nitrogen ligands, it is likely that the spectral changes were due to small positional variations of one of the axial ligands, probably a water molecule occupying the vacant position on the distal side of the porphyrin plane.

The spectra of ELP did not change in the presence of the substrates H_2O_2 and ABTS, except that a narrow line because of the expected formation of the ABTS radical was observed at $g = 2.0$ (Figure 6, line c). The spectra of compounds I and II could not be detected under our experimental conditions.

Intrinsic Fluorescence and CD Spectroscopy. ELP showed a fluorescence emission spectrum with a maximum at 336 nm when excited at 295 nm. The spectrum was independent of the presence of calcium ions. The CD spectra of native ELP show no significant modification upon addition of 10 mM Ca^{2+}, neither at 195 and 210 nm nor in the Soret region, indicating that gross changes in the secondary or tertiary structure did not occur (results not shown).

DISCUSSION

Monovalent and divalent metal cations have been found to activate or inhibit many enzymes. These cations can act as allosteric effectors without taking part in the reaction catalyzed by the enzyme or can exert a role by maintaining a specific protein structure conformation necessary for catalytic activity. For example, in HRP-C Ca^{2+} has been shown to play an important role in maintaining the protein structure in the heme microenvironment (*6*), and removal of the Ca^{2+} from the enzyme causes a loss of half of its enzymatic activity (*6*, *35*−*37*). Thus, Ca^{2+} ions are necessary for optimum catalysis but are not essential for lower levels of activity.

The results presented here show that a cationic peroxidase extracted from the latex of the perennial Mediterranean shrub *E. characias* has one strongly bound endogenous Ca^{2+} ion, as determined by atomic absorption measurements. Removal of that calcium ion after incubation with 6 M guanidine hydrochloride and 10 mM EDTA results in changes in electronic structure of the heme iron, and the activity of Ca-free enzyme was approximately 2% of the native enzyme. However, addition of a second Ca^{2+} ion to native ELP increased the enzyme activity 100 times with a drastic increase of k_{cat} and a decrease of K_M for hydrogen peroxide. The enzyme efficiency parameters k_{cat}/K_M increased almost 1000-fold as compared to the native enzyme. The activation was strongly pH-dependent, reaching its maximum at pH 5.75. An estimate of 1 mol of Ca^{2+} ion binding per mol of ELP was obtained by analyzing the dependence of k_{cat} on the concentration of Ca^{2+} ions; the activating effect disappears after dialysis or after gel filtration. Thus, we may conclude that one endogenous tightly bound Ca^{2+} represents an essential factor in maintaining the protein structure around the heme environment, as reported for class III peroxidases, whereas the second Ca^{2+} ion is loosely bound but acts as a potent activator.

Other divalent cations such as Sr^{2+} and Ba^{2+} gave rise to less activation of the enzyme, whereas Mg^{2+} and Mn^{2+} had no effect on ELP activity. Similar findings were reported for barley peroxidases (*9*); the lack of efficient activation by other metal ions might simply be related to the difference in ionic radii.

CN^- behaves as a competitive inhibitor of ELP. Since it is well-known that the cyanide adduct may be compared to the initial binding of hydrogen peroxide to peroxidases (*32*), it seemed worthwhile to analyze the influence of Ca^{2+} ions on the binding of cyanide. In the presence of Ca^{2+} the K_i value, at pH 5.75, was shown to be lower than in the native enzyme, demonstrating that the affinity for this anion is markedly changed after the binding of Ca^{2+}.

The determination of the rate constants of the single elementary steps of the catalytic cycle is difficult and model dependent; therefore, the data reported in Table 3 should be read with some caution. This said, it is obvious from our experiments that (i) the second-order rate constant for the formation of compound I (k_1) depends on calcium ions, being much faster in the presence of this ion, and (ii) the model of the catalytic cycle presented in Figure 4 is sufficient to account for the results obtained in the presence of calcium but not for those in its absence. Our analysis also suggest that the rate constants of other steps of the catalytic cycle may be affected by calcium, but in view of the poor fit of the kinetic model employed we cannot be confident on this point.

The laser photolysis results are compatible with the hypothesis that ferrous ELP presents two different structural conformations, characterized by different reactivities toward CO and that the equilibrium between them is shifted by the binding of Ca^{2+} ions. Since the apparent affinity of ELP for calcium ions is the same in these experiments and in steady-state measurements (carried out on the ferric enzyme and its higher oxidation states), we assume that the calcium-induced structural perturbations are independent of the oxidation state of the heme iron. It may seem paradoxical that the structural change favored by calcium ions makes ferric ELP more reactive toward hydrogen peroxide, whereas it makes the reduced enzyme less reactive toward CO. However, it should be considered that the ferric and ferrous iron have different atomic radii and different bond distances with the porphyrin nitrogens (*38*). Thus, the effect of the same structural perturbation may not necessarily be the same in reduced and oxidized ELP.

The results reported above indicate that the combination of enzyme with substrate (or cyanide) and with calcium are not independent so that the free enzyme and the enzyme−Ca^{2+} complex (E-Ca) have different affinities for the substrate. Thus, in the presence of Ca^{2+} ions the *Euphorbia* peroxidase is completely converted into the more active form ELP*-Ca^{2+}. This may be more generally described as a rearrangement in which ELP can adopt either of two different conformations, and calcium changes the equilibrium (see Scheme 1). The conformation indicated as ELP* in Scheme 1 may explain the effect of calcium on the affinity of ferric ELP for cyanide, the reaction with hydrogen peroxide, and the biphasic rebinding of CO to the reduced enzyme.

Neither the X-ray structure nor the amino acid sequence of ELP has been reported, so the local structure in the proximity of the distal and proximal Ca^{2+} binding sites is not known. UV/vis absorption spectra and CD measurements show that the heme iron of ELP is pentacoordinated high-spin. Since fluorescence and CD spectroscopy could not detect any modification of secondary and tertiary structure of ELP after addition of Ca^{2+}, the structural changes associated with activation by this effector must be quite subtle. This is by no means uncommon for hemoproteins, and indeed it occurs also in the case of the allosteric effectors of hemoglobin. Nevertheless, a significant change in the relaxation behavior of Fe^{3+} was detected by EPR after addition of Ca^{2+}, suggesting a change in the local geometry close to the iron.

Because of the lack of structural information, the effect of calcium ions on the kinetic and catalytic properties of ELP cannot be fully explained. Basically, two effects on the heme reactivity should be considered, both indirectly linked to calcium binding. Proximal effects are due to the position of the proximal histidine, the only amino acid residue directly bound to the heme iron. The position of the proximal histidine dictates the geometry of the heme (i.e., whether it is flat or domed), and as a consequence, its reactivity. Distal effects occur on the opposite side of the heme and may make the iron more or less accessible to a ligand or change the interactive strength of amino acids involved in the substrate activation. Although it is not easy to discriminate between

proximal and distal effects, it is unlikely that the ferric heme iron may be made unreactive toward hydrogen peroxide; therefore, we favor the hypothesis that the most relevant effect of calcium ions may be exerted on the distal residues of the heme pocket. This hypothesis is in keeping with the EPR data; however, the effects observed cannot be attributed with certainty to geometry changes at the distal side. In fact, it was recently demonstrated that structural changes on the proximal side of a peroxidase could affect the binding of Ca^{2+} to the distal site (*39*).

In conclusion, evaluation of the experimental data available in this work suggests that the endogenous proximal Ca^{2+} ion is strongly bound in *Euphorbia* peroxidase, and it plays a critical role for retaining the active site geometry. The loss of this proximal Ca^{2+} ion causes essentially a reversible inactivation. The distal Ca^{2+} appears to be located in a low affinity binding site but is necessary for expression of the full activity of the enzyme. The drastic enhancement of k_{cat}/K_M that this Ca^{2+} produces, together with the ease of its removal, suggests that the enzyme activity is regulated strictly by the presence of calcium. To our knowledge, ELP is the first peroxidase to display this type of extreme modulation, and considering that Ca^{2+} has a second messenger action in plants, this activation could be a control mechanism of ELP activity of physiological relevance. It is well-known that the formation rate of compound I in peroxidases depends on the catalytic reactivity of the distal histidine as a general acid−base catalyst. From the results obtained, we suggest that the reorientation of the distal histidine after addition of calcium ions, and the consequent increase in basicity induced by the rearrangement of the distal cavity, results in an increase of the k_1 value. Obviously, alternative mechanisms may also be hypothesized. A definitive explanation of the mode of activation of *Euphorbia* peroxidase will probably be established by site-directed mutagenesis and X-ray diffraction studies soon.

ACKNOWLEDGMENT

We are thankful to Prof. Alberto Boffi (University of Rome "La Sapienza") for useful advice about CD and fluorescence spectroscopy.

REFERENCES

1. Welinder, K. G. (1992) Superfamily of plant, fungal, and bacterial peroxidases, *Curr. Opin. Struct. Biol. 2*, 388−393.
2. Rasmussen, C. B., Henriksen, A., Abelskov, K., Jensen, R. B., Rasmussen, S. K., Hejgaard, J., and Welinder, K. G. (1997) Purification, characterization, and stability of barley grain peroxidase BP1, a new type of plant peroxidase, *Physiol. Plant. 100*, 102−110.
3. Welinder, K. G. (1985) Plant peroxidases. Their primary, secondary, and tertiary structures, and relation to cytochrome *c* peroxidase, *Eur. J. Biochem. 151*, 497−450.
4. Poulos, T. L., Edwards, S. L., Wariishi, H., and Gold, M. H. (1993) Crystallographic refinement of lignin peroxidase at 2 Å, *J. Biol. Chem 268*, 4429−4440.
5. Haschke, R. H., and Friedhoff, J. M. (1978) Calcium-related properties of horseradish peroxidase, *Biochem. Biophys. Res. Commun. 80*, 1039−1042.
6. Shiro, Y., Kurono, M., and Morishima, I. (1986) Presence of endogenous calcium ion and its functional and structural regulation in horseradish peroxidase, *J. Biol. Chem. 261*, 9382−9390.
7. Howes, B. D., Feis, A., Raimondi, L., and Indiani, C. (2001) The critical role of the proximal calcium ion in the structural properties of horseradish peroxidase, *J. Biol. Chem. 276*, 40704−40711.
8. Converso, D. A., and Fernandez, M. E. (1996) Ca^{2+} activation of wheat peroxidase: a possible physiological mechanism of control, *Arch. Biochem. Biophys. 333*, 59−65.
9. Rasmussen, C. B., Hiner, A. N. P., Smith, A. T., and Welinder, K. G. (1998) Effect of calcium, other ions, and pH on the reaction of barley peroxidase with hydrogen peroxide and fluoride, *J. Biol. Chem. 273*, 2232−2240.
10. Henriksen, A., Welinder, K. G., and Gajhede, M. (1998) Structure of barley grain peroxidase refined at 1.9-Å resolution, *J. Biol. Chem. 273*, 2241−2248.
11. Sutherland, G. R. J., Zapanda, L. S., Tien, M., and Aust, S. D. (1997) Role of calcium in maintaining the heme environment in manganese peroxidase, *Biochemistry 36*, 3654−3662.
12. Floris, G., Medda, R., and Rinaldi, A. (1984) Peroxidase from *Euphorbia characias* latex: purification and properties, *Phytochem. 23*, 953−956.
13. Gelotte, B. (1960) Studies on gel filtration sorption properties of the bed material Sephadex, *J. Chromatogr. 3*, 330−342.
14. Furhop, J. H., and Smith, K. M. (1975) Laboratory methods, in *Porphyrins and metalloproteins* (Smith, K. M., Ed.) pp 757−869, Elsevier, Amsterdam.
15. Dixon, M. (1953) The determination of enzyme inhibitor constants, *Biochem. J. 55*, 170−171.
16. Antonini, G., Bellelli, A., Brunori, M., and Falcioni, G. (1996) Kinetic and spectroscopic properties of the cyanide complex of ferrous hemoglobins I and IV from trout blood, *Biochem. J. 314*, 533−540.
17. Arcovito, A., Gianni, S., Brunori, M., Travaglini Allocatelli, C., and Bellelli A. (2001) Fast coordination changes in cytochrome *c* do not necessarily imply folding, *J. Biol. Chem. 276*, 41073−41078.
18. Wyman, J. (1948) Heme proteins, in *Advances in Protein Chemistry* (Anson, M. L., and Edsall, J. T., Eds.) pp 407−531, Academic Press Inc., New York.
19. Amiconi, G., and Giardina, B. (1981) Measurement of binding of non-heme ligands to hemoglobins, in *Methods of Enzymology* (Colowich, S. P., and Kaplan, N. O., Eds.) Vol. 76, pp 533−551 Academic Press, New York.
20. Blumberg, W. E., Peisach, J., Wittenberg, B. A., and Wittenberg, J. B. (1968) I. An electron paramagnetic resonance and optical study of horseradish peroxidase and its derivatives, *J. Biol. Chem. 243*, 1854−1862.
21. Roman, R., and Dunford, H. B. (1972) pH dependence of the oxidation of iodide by Compound I of horseradish peroxidase, *Biochemistry 11*, 2076−2083.
22. Yamada, H., and Yamazaki, I. (1974) Proton balance in conversions between five oxidation−reduction states of horseradish peroxidase, *Arch. Biochem. Biophys. 165*, 728−738.
23. Hewson, W. D., and Hager, L. P. (1979) Peroxidases, Catalases, and Chloroperoxidase, in *The Porphyrins* (Dolphi, D., Ed.) Vol XII, 295−335, Academic Press, New York.
24. Poulos, T. L., and Kraut, J. (1980) The stereochemistry of peroxidase catalysis, *J. Biol. Chem. 255*, 8199−8205.
25. Baek, H. K., and Van Wart, H. E. (1992) Elementary steps in the reaction of horseradish peroxidase with several peroxides: kinetics and thermodynamics of formation of compound 0 and compound I, *J. Am. Chem. Soc. 114*, 718−725.
26. Burner, U., and Obinger, C. (1997) Transient- and steady-state kinetics of the oxidation of aliphatic and aromatic thiols by horseradish peroxidase, *FEBS Lett. 411*, 269−274.
27. Isaac, I. S., and Dawson, J. H. (1999) Haem iron-containing peroxidases, in *Essays in Biochemistry* (Ballou, D. P., Ed.), Vol 34, pp 51−69, Portland Press, U.K.
28. Nakajima, R., and Yamazaki, I. (1987) The mechanism of oxyperoxidase formation from ferryl peroxidase and hydrogen peroxide, *J. Biol. Chem. 262*, 2576−2581.
29. Change, B., Powers, L., Ching, Y., Poulos, T., Schonbaum, G. R., Yamazaki, I., and Paul, K. G. (1984) X-ray absorption studies of intermediates in peroxidase activity, *Arch. Biochem. Biophys. 235*, 596−611.
30. Rodriguez-Lopez, J. N., Smith, A. T., and Thorneley, R. N. F. (1996) Role of arginine 38 in horseradish peroxidase, *J. Biol. Chem. 271*, 4023−4030.
31. Schonbaum, G. R., and Lo, S. (1972) Interaction of peroxidases with aromatic peracids, *J. Biol. Chem 247*, 3353−3360.

32. Rasmussen, C. B., Dunford, H. B., and Welinder, K. G. (1995) Rate enhancement of compound I formation of barley peroxidase by ferulic acid, caffeic acid, and coniferyl alcohol, *Biochemistry 34*, 4022−4029.
33. Hofrichter, J., Sommer, J. H., Henry, E. R., and Eaton, W. A. (1983) Nanosecond absorption spectroscopy of hemoglobin. Elementary processes in kinetic cooperativity, *Proc. Natl. Acad. Sci. U.S.A. 80*, 2235−2239.
34. Colvin, J. T., Rutter, R., Stapleton, H. J., and Hager, L. P. (1983) Zero-field splitting of Fe^{3+} in horseradish peroxidase and of Fe^{4+} in horseradish peroxidase compound I from electron sp relaxation data, *Biophys. J. 41*, 105−108.
35. Smith, A. T., Santama, N., Dacey, S., Edwards, M., Bray, R. C., Thorneley, R. N. F., and Burke, J. F. (1990) Expression of a synthetic gene for horseradish peroxidase C in *Escherichia coli* and folding and activation of the recombinant enzyme with Ca^{2+} and heme, *J. Biol. Chem. 265*, 13335−13343.
36. Ryan, O., Smyth, M. R., and Fágáin, C. O. (1994) Horseradish peroxidase: the analyst's friend, in *Essays in Biochemistry* (Tipton, K. F., Ed.), Vol 28, 129−146, Portland Press, Brookfield, VT.
37. Morishima, I., Kurono, M., and Shiro, Y. (1996) Presence of endogenous calcium ion in horseradish peroxidase, *J. Biol. Chem 261*, 9391−9399.
38. Perutz, M. F. (1979) Regulation of oxygen affinity of hemoglobin: influence of structure of the globin on the heme iron, *Annu. Rev. Biochem. 48*, 327−386.
39. Banci, L., Bertini, I., Capannoli, C., Del Conte, R., and Tien, M. (1999) Spectroscopic characterization of active mutants of manganese peroxidase: mutations of the proximal site affect calcium binding of the distal side, *Biochemistry 38*, 9617−9625.

BI034609Z